Biol. Cybern. 88, 459–467 (2003)
DOI 10.1007/s00422-003-0401-2

Biological Cybernetics

Stimulus-dependent onset latency of inhibitory recurrent activity

C. Hauptmann[1], **M. C. Mackey**[2]

[1] Centre for Nonlinear Dynamics in Physiology and Medicine, McGill University, 3655 Drummond Street, Montreal, Quebec, Canada H3G lY6
[2] Departments of Physiology, Physics, Mathematics & Centre for Nonlinear Dynamics in Physiology and Medicine, McGill University, 3655 Drummond Street, Montreal, Quebec, Canada H3G lY6

Received: 31 May 2002 / Accepted: 5 February 2003 / Published online: 20 May 2003

Abstract. This paper gives an explanation for the experimentally observed onset latencies of the inhibitory responses that vary from a few milliseconds to hundreds of milliseconds in systems where the conduction delays are only several milliseconds in the feedback pathways. To do this we use a simple mathematical model. The model consists of two delay differential equations (DDE) where the nonlinear relation between the postsynaptic potential and the firing frequency of the neuron population arises from the stoichiometry of the transmitter-receptor kinetics. The parameters of the model refer to the hippocampal feedback system, and the modeling results are compared with corresponding experiments.

1 Introduction

The process in neural circuits in which the activity of a neuron population excites a second population that in turn inhibits the first one is called recurrent inhibition. Recurrent inhibition is ubiquitous in the nervous system, occurring in insects through humans at levels from the spinal cord to the cortex, and is observed, for example, in the hippocampus (Andersen et al. 1964a,b; MacVicar and Dudek 1982) and incorporated in mathematical models, for example, by Wilson and Cowan (1972, 1973). Many investigators and research groups have contributed to the investigation of the functional role of recurrent inhibition, but its function remains obscure.

Time delays are a crucial element in recurrent inhibition and seem to play a major role in the control of the nervous systems. They are introduced by the synaptic time delays, conduction (propagational) delays (an der Heiden 1980; Marcus and Westervelt 1989; Destexhe and Babloyantz 1991; Liljenström 1991; Destexhe and Babloyantz 1992), and, as we investigate in this study, by the dynamical properties of the systems involved. Time delays may give rise to complex behavior (an der Heiden 1980; Mackey and an der Heiden 1984; Marcus and Westervelt 1989; Giannakopoulos et al. 2001a,b) and have strong effects on the timing of synchronized signals and thereby on the process of signal transmission (Traub and Miles 1991b; Hauptmann 2000; Giannakopoulos et al. 2001a). While time delays arise from the interconnection and communication of neuron populations, it is important to investigate the effects and sources of time delays starting with spatially localized neural populations.

In this paper, a simple model of recurrent inhibition and excitation is investigated. A variable and stimulus-dependent onset latency is observed in the model dynamics, and the results are compared with previous experimental observations.

The paper is structured as follows. The model is presented and developed in Sect. 3.2. For a specific example – the CA3 region of the hippocampus – the model parameters are estimated in Sect. 3.1. In Sects. 3.2 and 3.3, the dynamical behavior, and especially the stimulus amplitude-dependent onset latency of the inhibitory response, is investigated. The duration and amplitude of the inhibition induced by stimulation of a neuron population out of a neuronal network are investigated in Sect. 3.4. The results are discussed in Sect. 3.4.

The intention of the paper is to show that the dynamical properties of the interconnected neuron populations may be responsible for the stimulus-dependent onset latency of the recurrent inhibitory response. Experimental results from intracellular and extracellular recordings from hippocampal slice preparations (Andersen et al. 1964a) are used to test whether the simulation results agree with the experimental data. The effect of latencies induced by the dynamical properties of the system is a general one, and it is assumed that the results in this paper also hold for other brain areas with similar connectivities and receptor kinetics.

Correspondence to: C. Hauptmann
(e-mail: chauptma@cnd.mcgill.ca)

2 The mathematical model

Numerous studies have developed mathematical models for recurrent inhibition (Milton 1996). In these models, one can find highly simplified models resulting from sophisticated assumptions and other models including innumerable physiological details.

The model used in this study is a modification of the model studied by Mackey and an der Heiden (1984). The model equations describe the dynamical behavior of spatially localized neural populations as considered by Wilson and Cowan (1972). In this model, the membrane potential of a postsynaptic neural population is controlled by the excitatory and inhibitory inputs, while the inhibitory inputs are a consequence of a recurrent inhibition pathway. The spiking behavior of the neurons is modeled by a membrane-potential-dependent firing-frequency function. It is assumed that the firing frequency of the inhibitory neuron population is proportional to the (time-delayed) firing frequency of the excitatory neuron population. This assumption permits the use of only one differential equation. The nonlinear interaction between the neuron populations considers the stoichiometry of the GABA receptor interaction.

Here, as a modification of the model (Mackey and an der Heiden 1984), an excitatory feedback pathway is added and the dynamics of the inhibitory neuron population are represented by a separate differential equation. We show that the onset latency is influenced by the dynamical properties of the inhibitory neuron population. The excitatory feedback pathway reflects excitatory self-coupling as well as excitatory connections to the other neuron populations, as shown schematically in Fig. 1.

2.1 The neuron model

The model consists of two equations, one for the excitatory population and one for the inhibitory population.

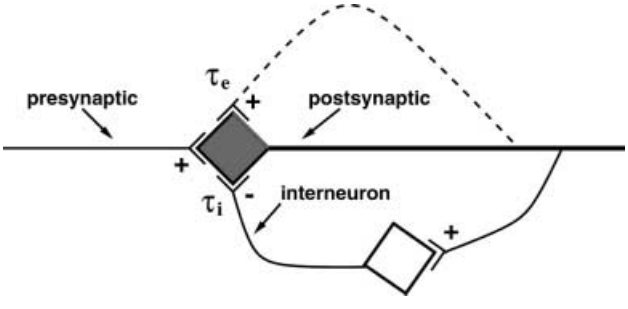

Fig. 1. Schematic picture of the modified model with recurrent inhibition and excitation. The excitatory (inhibitory) neuron population is indicated by the *shaded (white) square*. The additional excitatory feedback loop is drawn as a self-excitation (*dashed line*) and also represents the excitatory influences from neighboring neural populations. Both excitatory feedback loops branch off the outgoing fiber (*thick line*) of the excitatory neuron

$$\begin{aligned}\frac{dV_e(t)}{dt} &= \gamma_e(E - V_e(t)) - v_i\eta_i(\tilde{F}_i) + v_e\eta_e(\tilde{F}_e)\\ \frac{dV_i(t)}{dt} &= -\gamma_i V_i(t) + v_e\eta_e(\tilde{F}_e)\end{aligned} \tag{1}$$

where $v_{i/e}\eta_{i/e}(\tilde{F}_{i/e})$ denotes the excitatory/inhibitory feedback induced by the excitatory/inhibitory synaptic coupling, $V_{i/e}(t)$ denotes the membrane potential at time t for the excitatory/inhibitory neuron population, $\gamma_{i/e}$ is the inverse of the characteristic time constant of the synaptic interaction, E is a constant excitatory activation potential, and $\eta_{i/e}(\tilde{F}_{i/e})$ is a frequency-dependent interaction coefficient given by

$$\begin{aligned}\eta_i(\tilde{F}_i) &= R_i\Delta_i\frac{(m_i\tilde{F}_i(V_i))^{n_i}}{K_i + (m_i\tilde{F}_i(V_i))^{n_i}}\\ \eta_e(\tilde{F}_e) &= R_e\Delta_e\frac{(m_e\tilde{F}_e(V_e))^{n_e}}{K_e + (m_e\tilde{F}_e(V_e))^{n_e}}\quad .\end{aligned} \tag{2}$$

where $\Delta_{i/e}$ is the magnitude of postsynaptic potential induced by the activation of one excitatory/inhibitory receptor, R_e is the total number of excitatory receptors on a pyramidal cell in the hippocampal CA3 region, R_i is the corresponding number of receptors for the interneuron, and $m_{i/e}$ is a proportionality constant. For more details see below.

The frequency of action potentials generated in the excitatory and inhibitory neuron population is given by

$$\begin{aligned}\tilde{F}_{i/e}(V_{i/e}) = \kappa_{i/e}(V_{i/e}(t - \tau_{i/e}) - \Theta_{i/e}) \cdot\\ H(V_{i/e}(t - \tau_{i/e}) - \Theta_{i/e})\ ,\end{aligned} \tag{3}$$

where $H(x)$ is the Heavyside function, $\Theta_{i/e}$ is the activation threshold for firing, and $\tau_{i/e}$ is the time delay on the feedback pathway. For more details on the modeling of the inhibitory feedback see Mackey and an der Heiden (1984) and the corresponding modeling of the excitatory feedback below.

The parameters $v_{i/e}$ are the inverse of the onset and decay-time constants of the synaptic action and are assumed to be equal to $\gamma_{i/e}$, hence $v_{i/e} = \gamma_{i/e}$.

The frequency-dependent interaction coefficient $\eta_e(\tilde{F}_{i/e})$ relates the firing frequency to the amplitude of the induced excitatory postsynaptic potential and reflects the transmitter-receptor interaction and thus the effect of activation of excitatory receptors at the postsynaptic membrane. In the following, we discuss the transmitter-receptor reaction for the excitatory glutamate receptors. Through the function η_e the stoichiometry and the nonlinearity of the AMPA (α-Amino-3-hydroxyl-5-methyl-4-isoazolepropiomic acid) and NMDA (N-methyl-D-aspartate) receptor-mediated excitatory feedback enters the problem (Colquhoun et al. 1992). The transmitter interacting with the receptors is glutamate. The transmitter-receptor interaction is described by the chemical reaction equation

$$M_e + n_eC_e \rightleftharpoons L_e\ , \tag{4}$$

where n_e is the number of transmitter molecules required to activate one excitatory receptor, M_e is the number of

the receptors available for activation, C_e is the number of neurotransmitter (glutamate) molecules, and L_e is the number of activated receptors. Three assumptions allow us to calculate the fraction of active receptors:

– the transmitter-receptor reaction is rapid,
– there is a conservation of receptors so $R_e = L_e + M_e$, and
– there is no depletion of glutamate molecules.

The last assumption indicates that the synaptic pool of excitatory transmitter molecules is large. From Eq. 4 we get a differential equation for the change in the number of active receptors:

$$\frac{\mathrm{d}L_e}{\mathrm{d}t} = -k_1(L_e) + k_2 M_e C_e^{n_e} \quad , \tag{5}$$

where k_1 and k_2 are the reaction constants for Eq. 4. The steady-state solution gives the fraction of activated receptors:

$$G_e(L_e) = \frac{L_e}{R_e} = \frac{[C_e]^{n_e}}{K_e + [C_e]^{n_e}} \quad , \tag{6}$$

where $K_e = k_1/k_2$ and $[C_e]$ is the concentration of excitatory transmitter. The relation between the released transmitter concentration $[C_e]$ and the firing frequency $F(V)$ at the synaptic terminals of the neuron is assumed to be given by $[C_e] = m_e F(V)$, where m_e is a proportionality constant. For $G_e(F)$ we obtain

$$G_e(\tilde{F}_e) = \frac{(m_e \tilde{F}_e(V_e))^{n_e}}{K_e + (m_e \tilde{F}_e(V_e))^{n_e}} \tag{7}$$

The frequency-dependent interaction coefficient η_e is then given by

$$\eta_e = R_e \Delta_e G_e(\tilde{F}_e) \tag{8}$$

where R_e is the total number of excitatory receptors on a pyramidal cell in the hippocampal CA3 region and Δ_e is the magnitude of postsynaptic potential induced by the activation of one excitatory receptor.

Hence, for the modeling of the activation of receptors by the neurotransmitters released by action potentials we use the fraction of activated receptors

$$G_e(\tilde{F}_e) = \frac{(m_e \tilde{F}_e(V_e))^{n_e}}{K_e + (m_e \tilde{F}_e(V_e))^{n_e}} \tag{9}$$

for the excitatory glutamate receptors and

$$G_i(\tilde{F}_i) = \frac{(m_i \tilde{F}_i(V_i))^{n_i}}{K_i + (m_i \tilde{F}_i(V_i))^{n_i}} \tag{10}$$

for the inhibitory GABA receptors.

Next we need to estimate the following parameters for the excitatory feedback pathway:

– $\tau_{i/e}$: the delay time for the monosynaptic excitatory and inhibitory connections
– R_e: the average number of excitatory receptors per excitatory cell
– Δ_e: magnitude $[mV]$ of the excitatory postsynaptic potential resulting from the activation of one receptor
– n_e: number of neurotransmitter molecules required for activation of one receptor
– m_e: proportionality constant, gives the concentration of transmitter molecules released per action potential
– K_e: the equilibrium binding constant between excitatory transmitter molecules and excitatory cell receptors

With these parameters and the parameters estimated in Eurich et al. (2002) for the inhibitory feedback pathway and for the other model parameters all parameters of the model equations are determined.

As an example and to compare the simulation results with experimental studies, we will tailor the parameter estimation for the CA3 region of the hippocampus. The model is very simple compared to other models describing hippocampal dynamics; for example, see the complex models for hippocampal activity used by Traub and Miles (1991a,b). Since we discuss possible mechanisms for the origin of the onset latency of the inhibitory response induced by excitatory stimulation, it seems to be reasonable to us to use a simple model.

3 A specific example – the CA3 region of the hippocampus

3.1 Parameter estimation for the two-equation model of recurrent excitation and inhibition

The time delay τ The time delay $\tau_{i/e}$ is assumed to be equal for all three synaptic couplings, $\tau_{i/e} = \tau$. The feedback pathways are modeled as if they are monosynaptic. In a first experimental study of recurrent excitation between pyramidal cells in the CA3 region of the hippocampus, evidence was found for the existence of excitatory feedback, whereas the onset latency was found to be 2–4 ms (Lebovitz et al. 1971). These experiments were carried out using extracellular stimulation and recording, and spike latencies were studied relative to the onset of the antidromic field potential. A more recent study using simultaneous intracellular stimulation and recording of two neighboring pyramidal cells in the CA3 region of the rat hippocampus indicates that there is a nonzero probability of monosynaptic recurrent excitatory pathways between pyramidal cells. The observed latency may be as short as 0.5 ms (MacVicar and Dudek 1982; see also the experimental study of Miles and Wong 1986) (latency $\approx$ 1.0 ms).

Where populations of neurons are concerned we take

$$\tau = 2.0 \text{ ms} \tag{11}$$

for all three synaptic connections. This value takes into account the time delay due to the synaptic transmission ($\approx$ 1.0 ms) and a short propagation time ($\approx$ 1.0 ms) (Andersen et al. 1964a; Finch et al. 1988) that corresponds to a distance between the excitatory and inhibitory neuron population and a length of the self-

excitation pathway of $\approx 500\,\mu$m and an action potential propagation speed of 0.5 m/s. Note that in the experiments described in Andersen et al. (1964a), even for a very strong stimulation of local afferent fibers a minimal latency of 4.0 ms was observed, which corresponds to twice the conduction and synaptical delay of $\tau = 2.0$ ms.

The magnitude of the postsynaptic potential Δ_e In the literature, a large number of investigations deal with the magnitude of unitary synaptic events at hippocampal synapses induced by the stimulation of a single afferent fiber. The excitatory connections between CA3-CA3 are discussed and investigated in detail in the book by Traub and Miles (1991b). These connections reflect our model situation the best, and the values of the unitary events vary between 0.2 and 2.3 mV. The average magnitude of the EPSP is 1.3 mV, and we take this value for our simulations:

$$\tilde{\Delta}_e = 1.3\text{mV} \quad . \tag{12}$$

Note that this value for the magnitude of a unitary event is the magnitude of an event caused by a single afferent stimulation, so a large number of receptors are involved in one of these events and not just one. We must keep this in mind for the estimation of the other parameters, especially for the number R_e of excitatory receptors on one excitatory cell.

The number of excitatory receptors on one excitatory cell R_e In Megías et al. (2001), the number of excitatory and inhibitory inputs to a single pyramidal cell is given. These numbers are different from the number of excitatory receptors R_e we must estimate. Hence we denote these new parameters as $\tilde{R}_{i/e}$. The numbers $\tilde{R}_{i/e}$ are given for the CA1 region of the hippocampus, and we assume they are also valid as an upper bound for the CA3 region. The number of inhibitory synapses $\tilde{R}_i = 1700$ given in Megías et al. (2001) was also used in previous modeling studies dealing with a parameter set related to the CA3 region (Mackey and an der Heiden 1984; Finch et al. 1988). The maximal number of excitatory synapses per cell is given by

$$\tilde{R}_e = 30.000 \tag{13}$$

and is used for our simulations as an upper bound for R_e.

Both $\tilde{\Delta}_e$ (as estimated above) and $\tilde{R}_e$ are synapse-related values and not receptor-related values, as noted in Sect. 2. The following argument shows that we can use these values for our model. If we knew the number j of receptors per synapse, this number could be used to calculate the number of receptors on an excitatory cell from the number of synapses on these cells by $R_e = j \times \tilde{R}_e$. For the magnitude of a receptor event related to the magnitude of a synaptic event we can take $\Delta_e = \tilde{\Delta}_e / j$. Here we assume that an afferent stimulus affects one synapse only. Hence the product $\Delta_e R_e = \tilde{\Delta}_e \tilde{R}_e$ is independent of the number of receptors at one synapse, and the synaptic values $\tilde{\Delta}_e$ and $\tilde{R}_e$ can be used. Thus we obtain

$$\Delta_e = 1.3 \text{ mV} \quad \text{and} \quad R_e = 30.000 \ . \tag{14}$$

While we take into account only a subset of all the connections among neurons, the value R_e gives us an upper bound for the number of synapses involved.

The number of neurotransmitter molecules required for activation of one receptor n_e Receptors in the family of ligand-activated channels, which include ACh, $GABA_B$, glycine, and glutamate receptors, consist of two or more different subunits and are called oligomers (see Nicholls 1992, Chapt. 9, p. 301).

The fast-reacting AMPA receptor, a glutamate receptor, is a tetramer, having four binding sites. The degree of openness of the channel depends on the number of bound molecules. The receptor is activated completely if four transmitter molecules are bound to its binding sites, so

$$n_e = 4 \tag{15}$$

For more details see Rosenmund (1998).

The equilibrium binding constant K_e The binding between the excitatory transmitter molecules and the excitatory receptors is characterized by a binding (affinity) constant K_e. Experimentally this value is determined by measuring the inhibition induced by an application of a given concentration of glutamate in the synaptic gap. The response to a 1-ms pulse of 1 mM glutamate is desensitized by a previously applied conditioning concentration of glutamate. The concentration of previously applied glutamate, where the response to the added glutamate pulse is half as strong as without previously applied glutamate, is denoted as the equilibrium binding constant K_e or half occupancy (K_{50}). From experiments using slice preparations from the CA3 hippocampal region using AMPA/KA-type glutamate receptor channels we obtain

$$K_e = (9.6\ \mu M)^{n_e} \tag{16}$$

For more details see Colquhoun et al. (1992, Fig. 15 and Table 1).

The proportionality constant m_e This constant gives the concentration of transmitter molecules released per action potential. From Traub and Miles (1991b) we have one action potential activating three quanta of transmitter-release sites, whereas one transmitter-release site contains 5000 molecules of glutamate. This means that 15,000 molecules are released by one action potential. From Edwards (1995) we have more information about the geometry of excitatory synapses. The terminal area is 0.181 μm^2 and the width of the synaptic cleft 0.02 μm and thus similar to the values used in Eurich et al. (2002) for inhibitory synapses. These values give a synaptic volume of 0.00362 μm^3. Now we can calculate the value of m_e.

Table 1. Parameters estimated for the modified model of two neuron populations with recurrent inhibition and excitation. For the inhibitory feedback loop this parameter estimation follows the modeling study done by Eurich et al. (2002)

Parameter	Units	Hippocampus value	Reference
γ_e	ms^{-1}	0.125	Traub and Miles (1991b)
γ_i	ms^{-1}	0.1	Traub and Miles (1991b)
E	mV	[0, 2.0]	free parameter
Δ_i	mV	1	Eurich et al. 2002
Δ_e	mV	1.3	Traub and Miles (1991b)
R_i	–	[0, 1700]	Megías et al. (2001)
R_e	–	[0, 30000]	Megías et al. (2001)
K_i	$(\mu M)^{n_i}$	5^{n_i}	Eurich et al. (2002)
K_e	$(\mu M)^{n_e}$	9.6^{n_e}	Colquhoun et al. (1992)
m_i	μM-sec	0.62	Eurich et al. (2002)
m_e	μM-sec	6.91	Traub and Miles (1991b); Edwards (1995)
n_i	–	3	Eurich et al. (2002)
n_e	–	4	Rosenmund et al. (1998)
κ_i	$(mV\ s)^{-1}$	20	Eurich et al. (2002)
κ_e	$(mV\ s)^{-1}$	20	Eurich et al. (2002)
τ	msec	2.0	Andersen et al. 1964a; Finch et al. (1988)
Θ_i	mV	2	Eurich et al. (2002)
Θ_e	mV	2	Eurich et al. (2002)
ν_e	ms^{-1}	0.125	Traub and Miles (1991b)
ν_i	ms^{-1}	0.1	Traub and Miles (1991b)

$$m_e = \frac{15000}{\text{volume}} \frac{\text{molecules}}{\mu m^3} = \frac{15 \times 10^{18}}{\text{volume}} \frac{\text{molecules}}{\text{litre}} \quad . \tag{17}$$

If the duration of one action potential is 1 ms, we have for m_e

$$m_e = \frac{25 \times 10^{-3}}{0.00362}\ \mu\text{Msec} = 6.91\ \mu\text{Msec} \tag{18}$$

Note that this value for the excitatory synapses is nearly ten times larger than the value for the inhibitory synapses used in Eurich et al. (2002). We assume that the thresholds for activation $\Theta_{i/e}$ in Eq. 3 are the same for the excitatory and inhibitory feedback.

The parameters used in the simulations are summarized in Table 1.

3.2 Dynamical behavior of the isolated two-population model

In this section, we investigate the principal dynamical behavior of the isolated populations of neurons as described by the model (Eq. 1). We observed three different parameter regimes where the system displays different dynamical behavior.

- For $E < \Theta_e$ a stationary solution with $V_e = E$ is observed.
  - Also, after strong perturbations the system returns back to the stationary solution.
- For $\Theta_e < E < \Theta^\star$ (in our case $\Theta^\star \approx 21.4$ mV) the system shows periodic solutions.
  - These periodic solutions represent bursting solutions in which the system switches periodically between spiking and quiescence.
  - For $E > \Theta_e$ the period of the bursting first decreases with increasing E. If E is increased further, the bursting period increases again until a new steady state with $V_e > \Theta_e$ is reached.
- For $E > \Theta^\star$ a stationary solution with $V_e > \Theta_e$ is observed.
  - This superthreshold stationary solution of the membrane potential corresponds to a spiking solution in terms of the firing frequency of the excitatory and inhibitory neuron populations.

These characteristics of the dynamical changes of the system indicate that a bifurcation has occurred, and, based on the work of Eurich et al. (2002), it is probably a Hopf bifurcation. Since we are interested in the onset latency of the inhibitory response, we will not investigate the periodic solutions of the system in more detail. The onset latency can be observed for $E < \Theta_e$, where the system shows a stationary solution and an appropriate stimulation causes V_e to cross the threshold Θ_e. After the onset of the inhibitory response the system returns to its stationary solution, as shown in Fig. 2. As initial conditions for the delayed differential equations in the regime $E < \Theta_e$ (all simulations) we use constant initial functions, namely, the steady states of the system, which is E for the excitatory neuron population and zero for the inhibitory one.

3.3 Stimulus-dependent latency in the two-population model

For different stimulation strengths the two-population model shows similar time shifts of the inhibitory response as observed in experimental studies (see, for example, Andersen et al. 1964a). The time for the onset of the inhibitory response is calculated from the difference between the starting time of the stimulation and the first time the inhibition in Eq. 1 for the excitatory neuron population is not equal to zero, $\nu_i \eta_i(\tilde{F}_i) \neq 0$ (see the lower plot of Fig. 2). The stimulus is applied by changing the parameter E in Eq. 1.

The shape of the latency curve for weak stimulation amplitude is induced by the excitatory self-coupling in

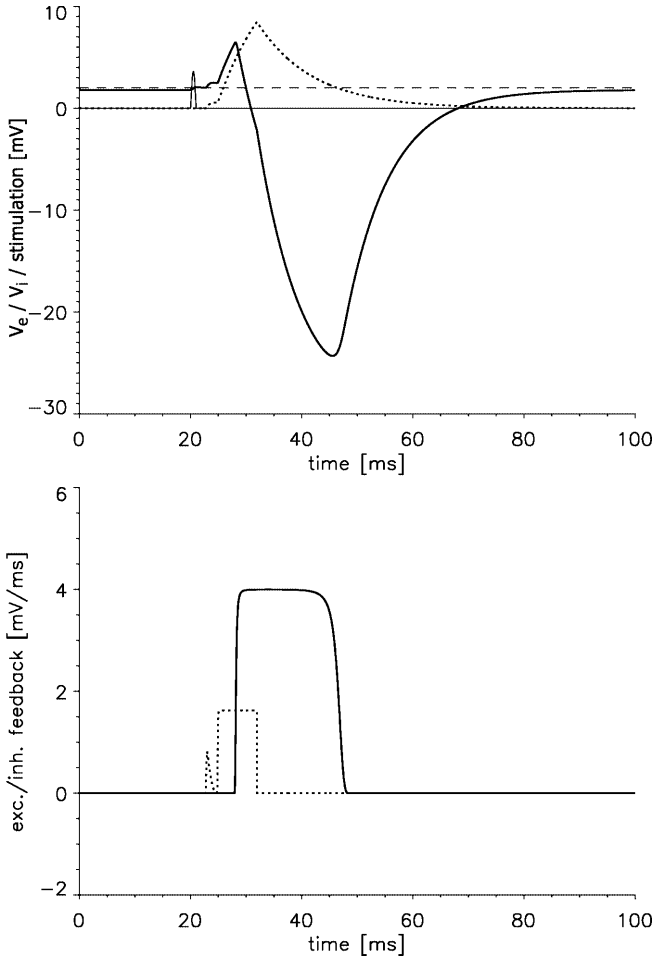

Fig. 2. Dynamical behavior of the stimulated system. Time course of the membrane potentials V_e (*thick line*) and V_i (*dotted line*) of the stimulated system. We used a sine-like stimulation (*thin line*) with amplitude 3.6 mV and a duration of 1 ms. The *dashed line* indicates the threshold $\Theta_{e/i}$ (*upper plot*). The excitatory response $v_e\eta_e(\tilde{F}_e)$ (*dotted line*) and the inhibitory response $v_i\eta_i(\tilde{F}_i)$ (*thick line*) are plotted in the *lower plot*. The inhibitory response starts after the membrane potential V_i has crossed the threshold Θ_i. Parameters: $E = 1.8$ mV, $R_e = 10$, $R_i = 40$

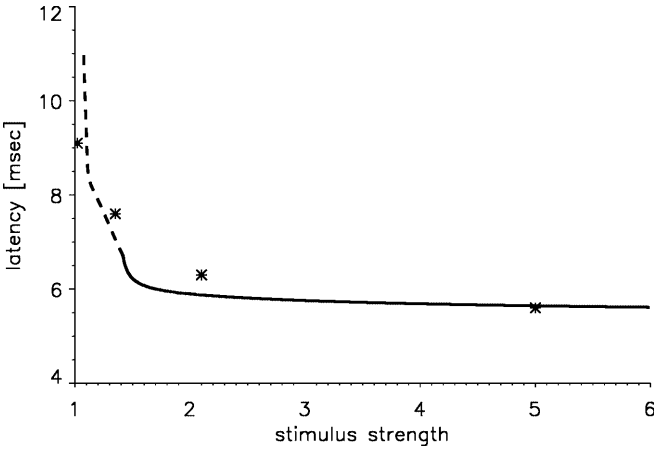

Fig. 3. Latency of the onset of the inhibitory response as a function of the stimulus strength. The stimulation is implemented by a sinusoidal-like peak with a duration of 1 ms. The *dashed branch* gives the latency curve observed for the system with excitatory self-coupling in the first equation of Eq. 1. Without excitatory self-coupling only the *solid branch* with a maximal latency of 6.73 ms is observed. The stimulation strength is scaled with a stimulation threshold of 3.0 mV. The experimentally observed data Andersen (1964a) are indicated by the stars. Parameters: $E = 1.8$ mV, $R_e = 10$, $R_i = 40$

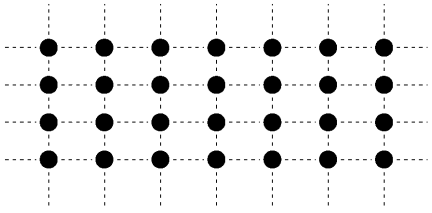

Fig. 4. Schematic diagram of the arrangement of the neuronal elements in the rectangular lattice. Each element gets input from the four neighboring elements; the coupling is an excitatory coupling. We use open boundary conditions

the equation for V_e (dashed branch in Fig. 3). Even weak stimulation can be amplified by this self-excitation while the inhibition is deactivated. During this amplification weak oscillations in V_e occur first (Fig. 2 upper plot). These weak oscillations are amplified by the excitatory self-feedback before these oscillations are able to activate the inhibitory subpopulation. The period of these oscillations is approximately 2.5 ms, and they are induced by a time delay of $\tau = 2.0$ ms. Without self-excitation a stronger stimulus is needed to result in an inhibitory response, and the long latency responses (latency larger then 6.5 ms) disappear (see Fig. 3).

3.4 Inhibitory response in a larger network of excitatory and inhibitory neuron populations

In this section, the inhibition is investigated in a network of 900 neuron populations in which nearest-neighbor connections exist among the excitatory neuron populations, as shown in Fig. 4.

The general structure of the network used in this paper follows the network structure developed in Traub and Miles (1991b). The neuron populations are arranged in a rectangular array of size $n \times n$. In neuronal networks, the probability of connections between neuron populations decreases with increasing distance between the populations, which was quantified for the rat visual cortex by Hellwig (2000) and holds for other neuronal areas too (Traub and Miles 1991b). In our case, we assume that the probability of finding a connection decreases rapidly enough to justify the simplification of nearest-neighbor connections. In this case, we can assume also that the propagational time delay and the connection strength are the same for all connections among the excitatory neuron populations. Hence, each excitatory neuron population from the neighborhood contributes $\frac{1}{4}$ of the total excitatory coupling strength, and there is no self-coupling of the excitatory neuron populations. The dynamics of the network are controlled by the following set of delayed differential equations:

$$\frac{dV_e^{i,j}}{dt} = \gamma_e(E - V_e^{i,j}) - S_i(V_i^{i,j}) + \frac{1}{4}[S_e(V_e^{i+1,j}) + S_e(V_e^{i,j+1}) + S_e(V_e^{i-1,j}) + S_e(V_e^{i,j-1})]$$
$$\frac{dV_i^{i,j}}{dt} = -\gamma_i V_i + S_e(V_e^{i,j}) \ , \tag{19}$$

where

$$S_i(V_i^{i,j}) = v_i \eta_i(\tilde{F}_i(V_i^{i,j}))$$
$$S_e(V_e^{i,j}) = v_e \eta_e(\tilde{F}_e(V_e^{i,j})) \ , \tag{20}$$

with

$$\tilde{F}_i(V_i^{i,j}) = \kappa_i(V_i^{i,j}(t - \tau_i) - \Theta_i)H(V_i^{i,j}(t - \tau_i) - \Theta_i)$$
$$\tilde{F}_e(V_e^{i,j}) = \kappa_e(V_e^{i,j}(t - \tau_e) - \Theta_e)H(V_e^{i,j}(t - \tau_e) - \Theta_e) \tag{21}$$

If an element from the center of the network is stimulated (stimulation amplitude 4.5 mV and duration 1 ms), the excitatory activity propagates within the network and is followed by a trailing inhibition front. The population activity shows a maximal network inhibition approximately 40 ms after the stimulation is applied (see Fig. 5). If the delay time for the network connections is increased, the excitation propagates with a lower velocity to the edges of the network. The largest number of inhibited neuron populations and the maximum of the inhibitory response in the network occur later than in the case with short delay, as we have shown in Fig. 5.

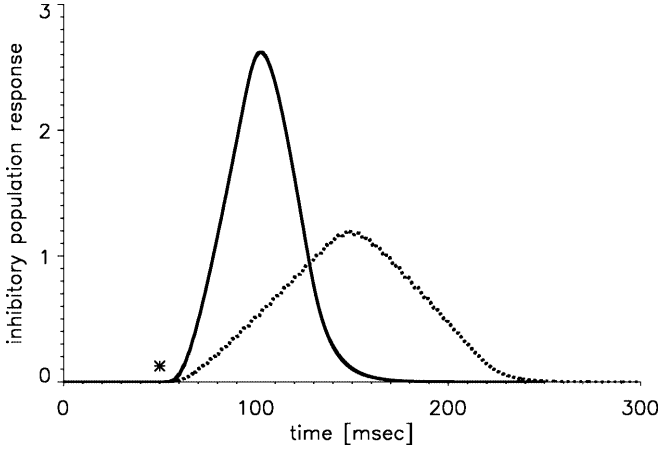

Fig. 5. Inhibitory response of the network. The stimulus is applied to one excitatory neuron population from the center of the network at 50 ms (indicated by the *star*). The long latency inhibitory response (*dashed line*) is a result of a simulation with a delay time of 5.0 ms for the network connections. Parameters: $E = 1.8$ mV, $R_e = 10$, $R_i = 40$

The activity pattern shown in Fig. 6 illustrates the reason for the dependence of the time of maximal inhibition on the network size. The activity propagates to the boundaries of the network and disappears due to the subsequent inhibition. The maximal total inhibition in the network is observed at the time when the largest number of neurons is inhibited strongly (see Fig. 6, third pattern from left).

These results confirm the existence of traveling front solutions originating from brief local stimulation as investigated in more detail by Jung and Mayer-Kress (1995), Wilson (1999), and Pinto and Ermentrout (2001). The slow local negative feedback results in traveling pulses. The traveling pulses create the certain shape of the inhibitory response of the network as seen in Figure 5.

If the network consists of 100 neuron populations only, the maximum of inhibition in the network is observed earlier, as shown in Fig. 7. The number of neuron populations inhibited at a given time is smaller and inhibited earlier than in the larger network, while the propagation speed of excitation within the network remains the same. Further simulations with networks of different sizes showed that the time to peak of the inhibitory response increases linearly with increasing numbers of neuron populations n in one row if an $n \times n$ network is simulated (see Fig. 8). The type of boundary condition does not strongly influence the time of maximal inhibition. We simulated the network with periodic boundary conditions and obtained qualitatively the same results (not illustrated). The network activity is terminated by the inhibitory activity induced by the excitatory activity.

4 Discussion

The model we have investigated is an extension of that of Mackey and an der Heiden (1984), which takes into account recurrent self-excitation via an additional variable controlled by a second differential equation. The modifications were carried out to show that long

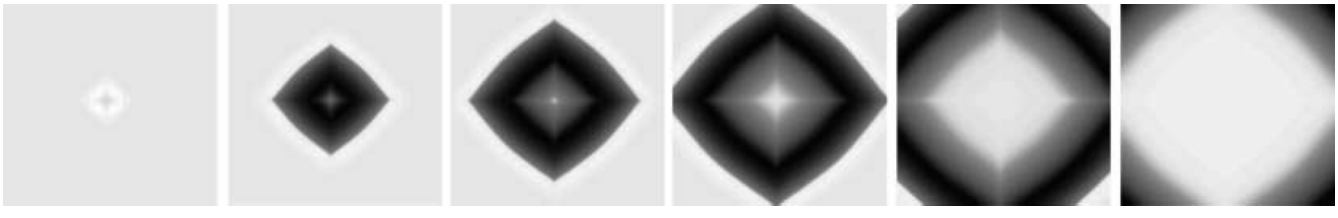

Fig. 6. Activity pattern of the network neuron populations. The different patterns correspond to the network activity 10, 30, 40, 50, 70, and 90 ms after the stimulation. The *gray scale* indicates the value of V_e, whereas *bright gray* indicates $V_e > E$ (excitation) and *darker gray* indicates $V_e < E$ (inhibition), where E is the steady-state value of the excitatory neuron populations. Here in all feedback pathways we assume a delay of 2.0 ms. Parameters: $E = 1.8$ mV, $R_e = 10$, $R_i = 40$

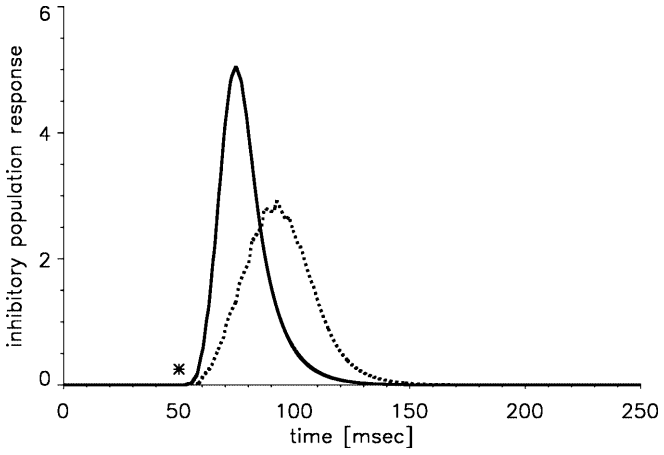

Fig. 7. Inhibitory response of the network with only 100 neuron populations. The stimulus is applied to one excitatory neuron population from the center of the network at 50 ms (indicated by the *star*). The long latency inhibitory response (*dashed line*) is a result of a simulation with a delay time of 5.0 ms for the network connections. Parameters: $E = 1.8$, $R_e = 10$, $R_i = 40$

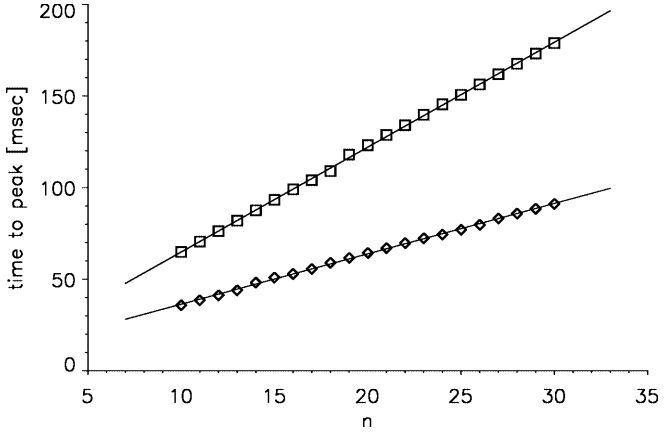

Fig. 8. Time to peak of the inhibitory network response as a function of the network size. The network size is given by the number of neuron populations in a row of the rectangular network n (an $n \times n$ network is simulated). The *diamonds* (*squares*) give the time to peak for the network simulations with short (long) connection delay. The slope of the *fitted line* is 2.75 (5.72)

latencies for the onset of the inhibitory response after stimulation of the excitatory neuron population can be introduced by the dynamical properties of the inhibitory neuron population.

The dynamical model for the inhibitory neuron population is similar to that of the excitatory neuron population. The total postsynaptic potential measured at the soma is controlled by a one-dimensional delay differential equation. To keep the model simple, we assumed that the sequence of action potentials could be mimicked by its firing frequency (see Mackey and an der Heiden 1984). If a threshold is crossed by the membrane potential, the neurons start to spike, whereas the firing frequency increases linearly with increasing membrane potential. The modeling structure of the excitatory interaction is the same as for the inhibitory interaction.

Stimulation of the excitatory neuron population results in an increase of the membrane potential of the excitatory neuron population, which in turn causes the onset of excitatory spiking. As a consequence, the inhibitory neuron population is stimulated and starts to spike if the activity is strong enough or lasts long enough. A positive inhibitory firing frequency then terminates the activity of the excitatory neuron population. This simple mechanism of recurrent inhibition includes the summation of stimulating signals in space and time, which is a consequence of the inertia of the differential equation and controlled by the damping constants $\gamma_{e/i}$. If the stimulation is weak or the damping is strong, the stimulation must last for a long time to cause an activation of the neuron population, which results in a stimulus amplitude dependence of the onset latency of the inhibitory activity. It is remarkable that connections formed by gap junctions with an extremely fast transmission time (no time delay) cannot reverse the effect of delays induced by the dynamical properties of the neuron population.

These results match with the results of the experimental study done by Andersen et al. (1964a), who showed in great detail the influence of the stimulation amplitude on the onset latency of the inhibitory response. They investigated the CA3 region of the cat hippocampus and applied a commissural stimulation. As a result they found onset latencies of the inhibitory response varying from 5.6 to 9.1 ms, while for increasing amplitude the onset latency gets shorter. On the other hand, a volley applied to an afferent pathway is able to inhibit the response of the pyramidal neurons to a test discharge for a long period, approximately 100–200 ms.

Our network simulations offer an explanation for this experimentally observed long-lasting inhibition in extended neuronal systems. Times to peak of 40–100 ms can occur when the time constants $\gamma_{e/i}$ are chosen to match the dynamics of fast excitatory and inhibitory synapses. The excitation propagates within the network and is terminated by a subsequent inhibition front. The maximal size of this inhibition front depends on the network size and stimulus location. This leads to another important result: the network size depends on the time evolution of the inhibitory reaction. Activity propagation in two-dimensional networks controls the shape and duration of the overall inhibition.

The results in this paper give a simple model-based demonstration of how the dynamical features of recurrent inhibition and excitatory feedback can induce stimulus-dependent onset latencies. These results may also be of use for future modeling studies where even more simplified models are used. If the dynamical behavior of the compartments of the model are restrained, it might be reasonable to consider the implementation of fixed time delays in the 5-to-10-ms range instead of only the conduction time delay of 2.0 ms.

Even though the proposed model is very simple and does not take into account the spiking of the neuron populations, it seems to be sufficient to explain the experimental results first observed by Andersen et al. (1964).

Acknowledgements. We thank Prof. Krnjevic and Prof. Glavinovic for helpful and extensive discussions about this problem. This work was supported by MITACS (Canada), the Natural Sciences and Engineering Research Council (NSERC grant OGP-0036920, Canada), the Alexander von Humboldt Stiftung, Le Fonds pour la Formation de Chercheurs et l'Aide à la Recherche (FCAR grant 98ER1057, Québec), and the Leverhulme Trust (U.K.).

References

An der Heiden U (1980) Analysis of neural networks. In: Lecture notes in biomathematics 35. Springer, Berlin Heidelberg New York

Andersen P, Eccles JC, Løyning Y (1964a) Location of postsynaptic inhibitory synapses on hippocampal pyramids. J Neurophysiol 27: 592–607

Andersen P, Eccles JC, Løyning Y (1964b) Pathways of postsynaptic inhibition in the hippocampus. J Neurophysiol 27: 608–619

Colquhoun D, Jonas P, Sakmann B (1992) Action of brief pulses of glutamate on AMPA/Kainate receptors in patches from different neurons of rat hippocampal slices. J Physiol 458: 261–287

Destexhe A, Babloyantz A (1991) Pacemaker-induced coherence in cortical networks. Neural Comput 3: 145–154

Destexhe A, Babloyantz A (1992) Cortical coherent activity induced by thalamic oscillations. In: Taylor JG, Caianiello ER, Cotterill RMJ, Clark JW (eds) Neural network dynamics. Springer, Berlin Heidelberg New York, pp 234–249

Edwards FA (1995) Anatomy and electrophysiology of fast central synapses lead to a structural model for long-term potentiation. Physiol Rev 75: 759–787

Eurich C, Mackey MC, Schwegler H (2002) Recurrent inhibition dynamics: the role of state dependent distributions of conduction delay times. J Theor Biol 216: 31–50

Finch DM, Tan AM, Isokawa-Akesson MI (1988) Feedforward inhibition of the rat entorhinal cortex and dubicular. J Neurophysiol 8: 2213–2226

Giannakopoulos F, Bihler U, Hauptmann C, Luhmann HJ (2001a) Epileptiform activity in a neocortical network: a mathematical model. Biol Cybern 85: 257–268

Giannakopoulos F, Hauptmann C, Zapp A (2001b) Bursting activity in a model of a neuron with recurrent synaptic feedback. Fields Inst Comm 29: 147–159

Hauptmann C (2000) Epileptiform activity in differential equation models of neuronal networks. PhD thesis, University of Cologne, Shaker, Aachen, Germany

Hellwig B (2000) A quantitative analysis of the local connectivity between pyramidal neurons in layers 2/3 of the rat visual cortex. Biol Cybern 82: 111–121

Jung P, Mayer-Kress G (1995) Noise controlled spiral growth in excitable media. Chaos 5: 458–462

Lebovitz RM, Dichter M, Spencer WA (1971) Recurrent excitation in the CA3 region of cat hippocampus. Int J Neurosci 2: 99–108

Liljenström H (1991) Modeling the dynamics of olfactory cortex using simplified network units and realistic architecture. Int J Neurol Syst 2: 1–15

Mackey MC, an der Heiden U (1984) The dynamics of recurrent inhibition. J Math Biol 19: 211–225

MacVicar BA, Dudek FE (1982) Local synaptic circuits in rat hippocampus: interactions between pyramidal cells. Brain Res 184: 220–223

Marcus CM, Westervelt RM (1989) Stability of analog neural networks with delay. Phys Rev A 39: 347–359

Megías M, Emri Z, Freund TF, Gulyás AI (2001) Total number and distribution of inhibitory and excitatory synapses on hippocampal CA1 pyramidal cells. Neuroscience 102: 527–540

Miles R, Wong RKS (1986) Excitatory synaptic interactions between CA3 neurons in the guinea-pig hippocampus. J Physiol 373: 397–418

Milton J (1996) Dynamics of small networks. American Mathematical Society, Providence, RI

Nicholls JG, Martin AR, Wallace BG (1992) From neuron to brain, 3rd ed. Sinauer Associates, Sunderland, MA

Pinto DJ, Ermentrout GB (2001) Spatially structured activity in synaptically coupled neuronal networks. I. Traveling fronts and pulses. SIAM J Appl Math 62: 206–225

Rosenmund C, Stern-Bach Y, Stevens CF (1998) The tetrameric structure of a glutamate receptor channel. Science 280: 1596–1599

Traub RD, Miles R (1991a) Mutliple modes of neuronal population activity emerge after modifying specific synapses in a model of the CA3 region of the hippocampus. Ann New York Acad Sci 627: 277–290

Traub RD, Miles R (1991b) Neural networks of the hippocampus. Cambridge University Press, Cambridge

Wilson H (1999) Spikes, decisions, and actions: the dynamical foundations of neuroscience. Oxford University Press, Oxford

Wilson HR, Cowan JD (1972) Excitatory and inhibitory interaction in localized populations of model neurons. Biophys J 12: 1–24

Wilson HR, Cowan JD (1973) A mathematical theory of the functional dynamics of cortical and thalamic nervous tissue. Kybernetik 13: 55–80